ISSN : 0974 - 7540 Volume 3 Issue 1

Trade Science Inc.

Research & Reviews On Electrochemistry

Full Paper

RREC, 3(1), 2012 [1-11]

3,4-Dimethoxybenzaldehydethiosemicarbazone as corrosion inhibitor for anneaed 18 Ni 250 grade maraging steel in 0.5 m sulphuric acid

T.Poornima[1], Jagannatha Nayak[2], A.Nityananda Shetty[3]*

[1]Department of Science and Humanities, PESIT Bangalore - 560 085, (INDIA)

[2]Department of Metallurgical and Materials Engineering, National Institute of Technology Karnataka, Surathkal, Srinivasnagar - 575 025, Karnataka, (INDIA)

[3]Department of Chemistry, National Institute of Technology Karnataka, Surathkal, Srinivasnagar - 575 025, Karnataka, (INDIA)

E-mail : nityashreya@gmail.com

Received: 8th January, 2010 ; Accepted: 18th January, 2010

ABSTRACT

The corrosion inhibition of the annealed 18 Ni 250 grade maraging steel in 0.5 M sulphuric acid by 3,4 dimethoxybenzaldehydethiosemicarbazone (DMBTSC) has been investigated by Tafel polarization and electrochemical impedance spectroscopy(EIS) techniques. The effect of concentration of inhibitor and solution temperature on inhibition efficiency of the inhibitor was studied. DMBTSC inhibits corrosion even at very low concentration. Polarisation curves indicate mixed type inhibition behavior affecting both cathodic and anodic corrosion currents. The mechanism of inhibition is discussed on the basis of an adsorption isotherm, and calculated thermodynamic parameters. Adsorption of DMBTSC on the annealed maraging steel surface is in agreement with the Langmuir adsorption isotherm model, and the calculated Gibb's free energy values confirm the chemical nature of the adsorption.

KEYWORDS

Inhibition;
Maraging steel;
Adsorption;
Cathodic reaction;
Polarization resistance.

INTRODUCTION

Corrosion of structural elements is a major issue for any industry because of the chemical environment of chemical processing. Corrosion Inhibition is one of the most important applications in corrosion protection. Inhibitors protect the metal by adsorbing onto the surface and retard metal corrosion in aggressive environment. Selecting the appropriate inhibitor for specific environment and metal is of great importance, since the inhibitor which protects one particular metal may accelerate the corrosion of another. Maraging steels are special class of ultra high strength steels that differ from conventional steels in that they are hardened by a metallurgical reaction that does not involve carbon[1]. They derive high strength from age hardening of low carbon, Fe-Ni martensitic matrix[2]. Recently, the needs of high reliable substances of high strength and high ductility are gradually increased with the development of aerospace industry. The characteristics of this grey and white steel are high ductility, formability, high corrosion resistance and high temperature strength, ease

of fabrication, weldability and maintenance of an invariable size even after heat treatment[3]. According to available literature, atmospheric exposure of 18 Ni maraging steel leads to corrosion in a uniform manner and become completely rust covered[4]. Pit depths tend to be shallower than high strength steels[5]. Bellanger et al[6] have studied the effect of slightly acid pH with or without chloride in radioactive water on the corrosion of maraging steel and have reported that corrosion behavior of maraging steel at the corrosion potential depends on pH, and intermediates remaining on maraging steel surface in the active region favoring the passivity. The effect of carbonate ions in slightly alkaline medium on the corrosion of maraging steel was determined by G Bellanger[7]. Heat treatment affects corrosion rate. Critical and passive current densities increase as the structure is varied from fully annealed to fully aged[8]. Maraging steels are found to be less susceptible to hydrogen embrittlement than common high strength steels owing to significantly low diffusion of hydrogen in them[9]. Several technical papers covering alloy design, material processing, thermo-mechanical treatments, welding, strengthening mechanisms, etc., have been published[10]. These steels have emerged as alternative materials to conventional quenched and tempered steels for advanced technologies such as aerospace, nuclear and gas turbine applications. They frequently come in contact with acids during cleaning, pickling, descaling, acidising, etc. Materials used in acid environment should have good corrosion resistance.

Thiosemicarbazones and their derivatives have continued to be subject of extensive investigation in chemistry and biology owing to their broad spectrum of anti-tumor[11,12], antimalarial[13] and many other applications including corrosion inhibition of metals[14,16]. The inhibiting action of thiosemicarbazone derivatives has been mainly attributed to adsorption of thiocarbonyl group on the surface of metal. These compounds can be adsorbed on metal surface through lone pairs of electrons present on nitrogen or sulphur atoms and also through pi electrons present in these molecules[17,20]. The present work is intended to study the corrosion inhibition of annealed 18 Ni 250 grade maraging steel in 0.5M sulphuric acid medium using DMBTSC inhibitor.

EXPERIMENTAL

Material

The maraging steel samples (M 250 grade) in annealed condition were taken from plates which were subjected to solution annealing treatment at 815 ± 5°C for 1 hour followed by air cooling. Percentage composition of 18 Ni 250 grade annealed maraging steel samples is given in TABLE 1. Cylindrical test coupons were cut from the plate and sealed with epoxy resin in such a way that, the area exposed to the medium is 0.503 cm^2. These coupons were polished as per standard metallographic practice, belt grinding followed by polishing on emery papers, finally on polishing wheel using levigated alumina to obtain mirror finish, degreased with acetone, washed with double distilled water and dried before immersing in the corrosion medium. The inhibitor 3, 4 dimethoxybenzaldehyde thiosemicarba-zone (DMBTSC) was synthesized in one step reaction of 3, 4 dimethoxybenzaldehyde with thiosemicarbazide[13].

TABLE 1 : Composition of the annealeded maraging steel specimen (weight percentage)

Element	Composition (%)	Element	Composition (%)
C	0.015	Ti	0.3-0.6
Ni	17-19	Al	0.005-0.15
Mo	4.6-5.2	Mn	0.1
Co	7-8.5	P	0.01
Si	0.1	S	0.01
O	30 ppm	N	30 ppm
H	2.0 ppm	Fe	Balance

Medium

Standard solution of sulphuric acid having concentration 0.5 M was prepared by diluting analar grade 98% sulphuric acid by using double distilled water. The solutions of inhibitor with 2 x 10^{-5} M, 4 x 10^{-5} M, 10^{-4} M, 2 x 10^{-4} M, 4 x 10^{-4} M and 8 x 10^{-4} M concentration were prepared in 0.5 M sulphuric acid. Experiments were carried out using calibrated thermostat at temperatures 30 °C, 35 °C, 40 °C, 45 °C, 50 °C (±0.5 °C)

Electrochemical measurement

1. Tafel polarisation studies

Electrochemical measurements were carried out by

using an electrochemical work station, Auto Lab 30 and GPES software. Tafel plot measurements were carried out using conventional three electrode Pyrex glass cell with platinum counter electrode and saturated calomel electrode (SCE) as reference electrode. All the values of potential are therefore referred to the SCE. Finely polished composite and base alloy specimens were exposed to corrosion medium of different concentrations of hydrochloric acid – sulphuric acid mixtures at different temperatures (30 °C to 50 °C) and allowed to establish a steady state open circuit potential. The potentiodynamic current-potential curves were recorded by polarizing the specimen to -250 mV cathodically and +250 mV anodically with respect to open circuit potential (OCP) at scan rate of 1 mV s^{-1}.

2. Electrochemical impedance spectroscopy studies (EIS)

The corrosion behaviors of the specimens of the composite and the base alloy were also obtained from EIS technique using electrochemical work station, Auto Lab 30 and FRA software. In EIS technique a small amplitude ac signal of 10 mV and frequency spectrum from 100 kHz to 0.01 Hz was impressed at the OCP and impedance data were analyzed using Nyquist plots. The charge transfer resistance, R_{ct} was extracted from the diameter of the semicircle in Nyquist plot.

In all the above measurements, at least three similar results were considered and their average values are reported.

RESULTS AND DISCUSSION

Tafel polarization measurement

The corrosion inhibition of annealed maraging steel was investigated in 0.5 M sulphuric acid containing various concentration of DMBTSC inhibitor at different temperatures using Tafel polarization technique. Figure 1 represents Tafel polarization curves of the specimen in 0.5 M sulphuric acid containing different concentration of inhibitor under study at 30 °C. The percentage inhibition efficiency (IE %) was calculated from expression (2)

$$IE\% = \frac{I_{corr} - I_{corr(inh)}}{I_{corr}} \times 100 \qquad (2)$$

where I_{corr} and $I_{corr(inh)}$ are corrosion current densities in the absence and in the presence of inhibitor respectively. The valuable potentiodynamic polarization parameters including corrosion potential (E_{corr}), corrosion current (I_{corr}), anodic and cathodic slopes (b_a and b_c), and inhibition efficiency (%IE) were calculated from Tafel plots and are summarized in TABLE 2. The polarization resistance (Rp) increased with increase in inhibitor concentration, suggesting a hindrance to charge transfer reaction (metal dissolution). The value of I_{corr} decreases with increase in the concentration of inhibitor.

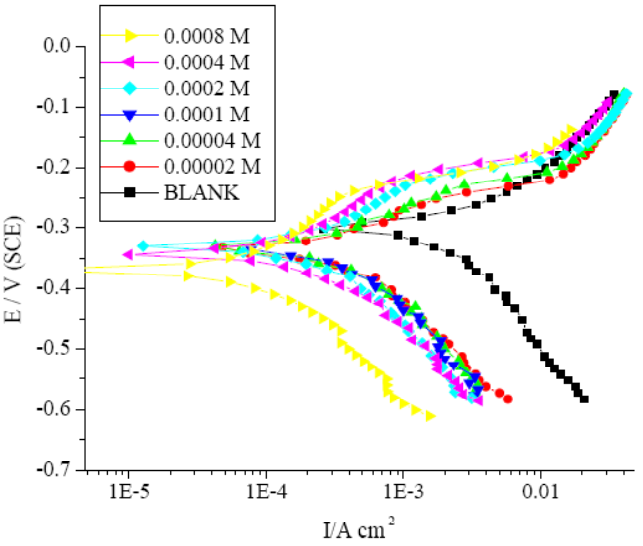

Figure 1 : Tafel polarization curves for the annealed maraging steel in 0.5 M sulphuric acid containing different concentrations DMBTSC.

As can be seen from the data, addition of DMBTSC decreases the corrosion of the annealed maraging steel sample. Inhibition efficiency increases with increasing DEABT concentration. The change in both the anodic and cathodic Tafel slopes observed on the addition of DMBTSC indicate that both anodic and cathodic reactions are affected by the addition of inhibitor. The addition of DMBTSC affects anodic dissolution of metal and also the hydrogen evolution reaction at the cathode.

No definite trend was observed in the shift of E_{corr} values, it can be recognized as an evidence for the mixed type inhibition by DMBTSC[21]. According to Ferreira and others[22,23], if the displacement in corrosion potential is more than ±85 mV with respect to corrosion potential of the blank, the inhibitor can be seen as a cathodic or anodic type. The data in the table reveal that

at lower concentrations of inhibitor, the shift in E_{corr} is very small, but the shift is relatively large to the negative direction at higher concentration. This indicates that DMBSCT acts as a mixed inhibitor with predominant cathodic action at higher concentrations.

The parallel cathodic Tafel curves suggest that the hydrogen evolution is activation controlled and the reduction mechanism is not affected by the presence of the inhibitors[21]. The values of b_c changed with increase in inhibitor concentration which indicates the influence of DMBTSC on the kinetics of hydrogen evolution. The shift in the anodic Tafel slope b_a may be due to the sulphate /or inhibitor molecules adsorbed on the steel surface[24].

TABLE 2 : Results of tafel polarization studies on annealed maraging steel in 0.5 M sulphuric acid containing various concentration of DMBTSC

Temperature (^{0}C)	Concentration of DMBTSC ($x10^{-4}$) (M)	E_{corr} (V)	$-b_c$ (V dec^{-1})	b_a (V dec^{-1})	I_{corr} ($x\ 10^{-4}$) (A cm^{-2})	%IE
30	0.0	-0.338	0.080	0.046	5.95	
	0.2	-0.335	0.160	0.070	2.20	63.4
	0.4	-0.332	0.139	0.093	2.05	65.7
	1.0	-0.327	0.137	0.097	1.70	71.4
	2.0	-0.331	0.127	0.095	1.23	79.6
	4.0	-0.342	0.092	0.136	1.03	83.6
	8.0	-0.370	0.097	0.122	0.45	92.8
35	0.0	-0.339	0.126	0.084	13.04	
	0.2	-0.331	0.193	0.108	2.80	78.3
	0.4	-0.338	0.177	0.097	2.27	82.6
	1.0	-0.340	0.131	0.103	2.05	85.0
	2.0	-0.329	0.118	0.103	1.44	88.9
	4.0	-0.349	0.132	0.132	1.18	91.1
	8.0	-0.375	0.100	0.132	0.45	95.7
40	0.0	-0.336	0.153	0.090	18.50	
	0.2	-0.336	0.159	0.118	4.41	79.5
	0.4	-0.331	0.158	0.108	2.90	84.9
	1.0	-0.335	0.141	0.084	2.38	87.7
	2.0	-0.334	0.129	0.111	1.64	91.6
	4.0	-0.353	0.148	0.128	1.25	92.9
	8.0	-0.381	0.127	0.139	0.65	94.7
45	0.0	-0.335	0.136	0.096	23.80	
	0.2	-0.334	0.142	0.087	3.93	81.7
	0.4	-0.330	0.103	0.071	3.43	86.6
	1.0	-0.333	0.120	0.100	2.90	89.0
	2.0	-0.344	0.087	0.073	2.09	91.7
	4.0	-0.363	0.119	0.144	1.76	92.5
	8.0	-0.388	0.113	0.124	1.45	94.4
50	0.0	-0.336	0.121	0.077	28.50	
	0.2	-0.331	0.113	0.089	4.07	83.8
	0.4	-0.344	0.098	0.089	3.78	88.5
	1.0	-0.336	0.116	0.084	3.28	90.4
	2.0	-0.356	0.128	0.129	2.33	92.5
	4.0	-0.384	0.113	0.091	2.17	94.3
	8.0	-0.381	0.134	0.128	1.30	95.6

Effect of temperature

The effect of temperature on the inhibited acid-metal reaction is highly complex because many changes occur on the metal surface, such as rapid etching and desorption of the inhibitor and the inhibitor itself, in some cases may undergo decomposition and/or rearrangement[25]. However it facilitates the calculation of many thermodynamic functions for the inhibition and/or the adsorption processes which contribute in determining the type of adsorption of the studied inhibitors. In the present study, with increase in solution temperature, corrosion potential (E_{corr}) and anodic Tafel slope (b_a), cathodic Tafel slope (b_c) values are not affected much. This indicates that increase in temperature does not change the mechanism of corrosion reaction. The I_{corr} and hence the corrosion rate of the specimen increases with increase in temperature in both blank and inhibited solutions. But inhibition efficiency increases with increase in temperature which is typical of chemisorption. According to Singh et al[26] with increase in temperature some chemical changes occur in the inhibitor molecules, leading to increase in the electron densities at the adsorption centers of the molecule, there by causing an improvement in inhibition efficiency.

The apparent activation energy (E_a) for the corrosion process in the presence and absence of inhibitor can be calculated using Arrhenius law equation 3[27].

$$\ln (C.R) = B - (E_a/RT) \quad (3)$$

where B is a constant which depends on the metal type and R is the universal gas constant. The plot of ln(corrosion rate) vs reciprocal of absolute temperature 1/T gives straight line whose slope = $-E_a/R$, gives activation energy for the corrosion process. The Arrhenius plots for the annealed specimen are shown in Figure 2. The Entropy and enthalpy of activation for the dissolution of alloy, (ΔH_a & ΔS_a) were calculated from transition state theory equation 3[28].

$$C.R = (RT/Nh) \exp(\Delta S_a/R) \exp(-\Delta H_a/RT) \quad (4)$$

where h is Plank's constant, N is Avagadro's number. A plot of ln(corrosion rate/T) vs 1/T gives straight line with slope = $-\Delta H_a/R$ and intercept = $\ln(R/Nh) + \Delta S_a/R$. The calculated values of ΔH_a and ΔS_a are given in TABLE 3. The plot of ln(corrosion rate/T) vs 1/T for annealed samples of maraging steel in various concentrations of inhibitor in 0.5 M sulphuric acid is shown in Figure 3.

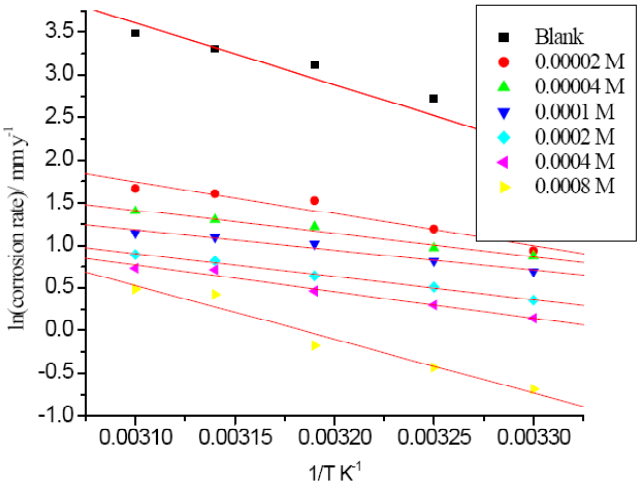

Figure 2 : Arrhenious plots for annealed maraging steel in 0.5 M sulphuric acid containing different concentrations of inhibitor.

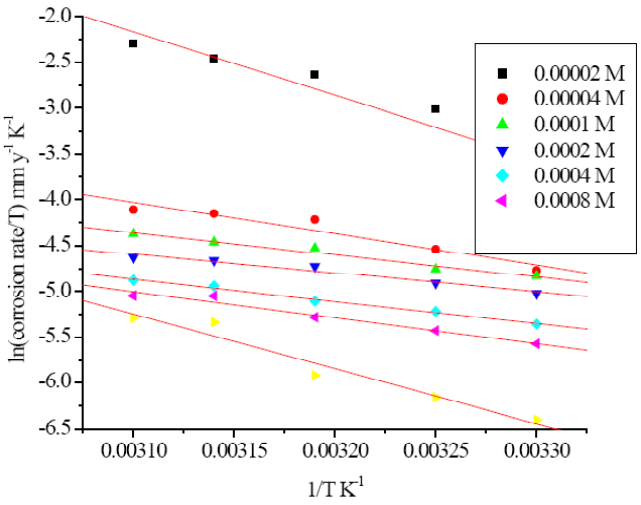

Figure 3 : ln(corrosion rate)/T vs 1/T for annealed maraging steel in 0.5M sulphuric acid containing different concentration of inhibitor.

The calculated values of activation parameters are given in TABLE 3.

The value of activation energy (E_a) in the presence of inhibitor is lower than in the absence of inhibitor indicating the possibility of increase in corrosion current in the presence of inhibitor, but corrosion current decreases in the presence of inhibitor. There must be change in mechanism of the corrosion process when inhibitor is used. It is attributed to be due to the chemical nature of interaction between inhibitor molecule and the steel surface as reported by Lagrenee et al[29]. The entropy of activation in the absence and presence of inhibitor is large and negative. This implies that the activated complex in the rate determining step represents an association rather than dissociation step, indicating that a decrease in disordering takes place on going from reactants to activated complex[30,31].

TABLE 3 : Activation parameters for the corrosion of annealed maraging steel in 0.5M sulphuric acid containing different concentration of DMBTSC.

Concentration ($x10^{-4}$) (M)	E_a (kJ mol^{-1})	ΔH_a (kJ mol^{-1})	ΔS_a (J mol^{-1})
0.0	60.11	57.51	-37.27
0.2	30.66	28.06	-144.14
0.4	22.40	19.86	-172.28
1.0	19.39	16.79	-183.73
2.0	22.54	19.94	-176.23
4.0	26.05	23.45	-166.50

Adsorption isotherm

Organic corrosion inhibitors are known to decrease metal dissolution via adsorption on the metal/corrodent interface to form a protective film which separates the metal surface from the corrosive medium. The adsorption route is usually regarded as a substitution process between the organic inhibitor in the aqueous solution [$Inh_{(sol)}$)] and water molecules adsorbed at the metal surface [$H_2O_{(ads)}$] as follows[32]:

$$Inh_{(sol)} + \chi H_2O_{(ads)} \leftrightarrow Inh_{(ads)} + \chi H_2O_{(sol)} \quad (5)$$

where χ represents the number water molecules replaced by one molecule of adsorbed inhibitor. The adsorption bond strength is dependent on the composition of the metal, corrodent, inhibitor structure, concentration and orientation as well as temperature. Basic information on the interaction between the inhibitor and alloy surface can be provided by adsorption isotherm. In order to obtain isotherm, the linear relation between surface coverage (θ) value and C_{inh} must be found. Attempts were made to fit the è values to various isotherms including Langmuir, Temkin, Frumkin and flory- Huggins

Full Paper

isotherms. By far the best fit is obtained with the modified Langmuir adsorption isotherm. The Langmuir isotherm for monolayer chemisorption is given by equation (6),

$$\frac{C_{inh}}{\theta} = \frac{1}{K} + C_{inh} \quad (6)$$

where C_{inh} is the concentration of inhibitor, K is the equilibrium constant for adsorption process, and θ is the degree of the surface coverage which is calculated using equation (7).

$$\theta = \frac{IE\%}{100} \quad (7)$$

where IE% is percentage inhibition efficiency as calculated using equation (2).

This model has also been used for other inhibitor systems[32,34]. The plots of C_{inh}/θ vs C_{inh} yields a straight line with intercept 1/K as shown in Figure 4.

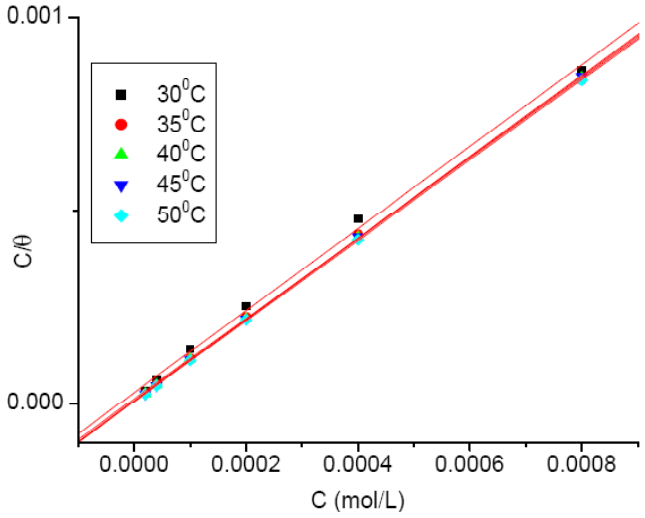

Figure 4 : Langmuir adsorption isotherm of DMBTSC on aged maraging steel in 0.5M sulphuric acid at different temperatures.

The values of standard free energy of adsorption are related to K by the relation (8).

$$K = \frac{1}{55.5} e^{\left(\frac{\Delta G^0_{ads}}{RT}\right)} \quad (8)$$

where the value 55.5 is the concentration of water in solution in M (mol/L), R is the universal gas constant and T is absolute temperature[35,37]. The values of ΔG^0_{ads} obtained from adsorption isotherms are depicted in TABLE 4. The correlation coefficient (R^2) was used to choose the isotherm that best fit experimental data[25].

The linear regression coefficients are close to unity and the slopes of straight lines are nearly unity, suggesting that the adsorption of DMBTSC obeys Langmuir's adsorption isotherm for monolayer chemisorption and there is negligible interaction between the adsorbed molecules[23]. The high values of K for the studied inhibitor indicate strong adsorption of inhibitor on the alloy surface. Negative values of ΔG^0_{ads} are characteristic feature of strong spontaneous adsorption for the studied compounds, which also reflect the high values of inhibition. The ΔG^0_{ads} values calculated from equation (7) are consistent with the spontaneity of the adsorption process and the stability of the adsorbed layer on the carbon steel surface. Generally the energy values of -20 kJ/mol^{-1} or less negative are associated with an electrostatic interaction between charged molecules and charged metal surface, physisorption, those of -40 kJ mol^{-1} or more negative involve charge sharing or transfer from the inhibitor molecules to the metal surface to form a coordinate covalent bond, chemisorption[38,39]. The ΔG^0_{ads} values obtained for the studied inhibitor on the annealed maraging steel surface in 0.5 M sulphuric acid are around -40 kJ/mol. This is an evidence for chemical adsorption. This observation is consistent with increase in inhibition efficiency with temperature and decrease in activation energy in the presence of inhibitor; both of these aspects indicate chemisorption. The unshared electron pairs in sulphur interact with d- orbitals of iron to provide a protective chemisorbed film at higher temperature.

A plot of ΔG^0_{ads} versus T in Figure 5 was used to

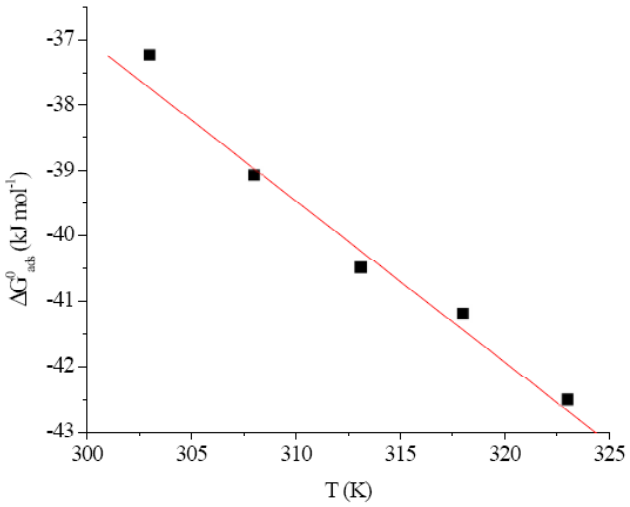

Figure 5 : Plot of ΔG^0_{ads} versus temperature in K

calculate heat of adsorption ΔH^0_{ads} and the standard adsorption entropy ΔS^0_{ads} according to the thermodynamic equation

$$\Delta G^0_{ads} = \Delta H^0_{ads} - T\,\Delta S^0_{ads} \quad (9)$$

The Figure clearly shows that the good dependence of ΔG^0_{ads} on T, indicating good correlation among thermodynamic parameters. The thermodynamic data obtained for DMBTSC using Langmuir adsorption isotherm are listed in TABLE 4.

The values of thermodynamic parameters for the adsorption of inhibitors can provide valuable information about the mechanism of corrosion inhibition. While an endothermic adsorption process ($\Delta H^0_{ads} > 0$) is attributed unequivocally to chemisorption[40], an exothermic adsorption process ($\Delta H^0_{ads} < 0$) may involve either physisorption or chemisorption or a mixture of both the processes. In the presemted case, the calculated values of ΔH^0_{ads} of DMBTSC IS 39.239 k J mol^{-1} indicating that this inhibitor can be considered chemically adsorbed. The ΔS^0_{ads} values in the presence of DMBTSC is large and positive, meaning that an disordering takes place in going from reactants to the metal adsorbed species reaction complex[41].

TABLE 4 : Thermodynamic parameters for the adsorption of DMBTSC on annealed maraging steel surface in 0.5 M sulphuric acid at different temperatures.

Temperature ^0C	K ($\times 10^4$) (M^{-1})	$-\Delta G^0_{ads}$ kJ mol^{-1}	R^2	ΔH^0_{ads} kJ mol^{-1}	ΔS^0_{ads} J mol^{-1} K^{-1}
30	47176	37.229	0.998		
35	111562	39.398	0.999	39.23	253.4
40	188228	40.715	0.999		
45	227130	41.189	0.999		
50	245902	42.389	0.999		

Electrochemical impedance spectroscopy

The results of potentiodynamic polarization experiments were with the results of impedance measurements, since EIS is a powerful technique in studying corrosion mechanism. In order to get more information about the corrosion inhibition of annealed maraging steel specimens in 0.5 M sulphuric acid containing DMBTSC, EIS measurements were carried out at different temperatures and they are displayed as Nyquists plots in the present study. The Nyquist plots obtained for annealeded samples of maraging steel specimens in 0.5 M sulphuric acid containing various concentrations of DMBTSC are as shown in Figure 6 and Figure 7 respectively. The impedence spectra contains a high frequency capacitive semicircle and low frequency inductive loop as shown in Figure 5. The impedance spectra in the presence of different concentration of DMBTSC are similar in shape with only high frequency semicircle whose diameter increases with increase in inhibitor concentration. The time constant at high frequency has often been attributed to formation of surface film or the surface film itself[42,43]. The inductive loop on the other hand has been attributed to a surface or bulk relaxation process or to a dissolution process[44,45]. In the present case the low frequency inductive loop observed only in the uninhibited acid medium,can be attributed to the surface dissolution process. The fact that this inductive lop can not be observed after the addition of inhibitor supports this view. DMBTSC inhibits corrosion by inhibiting the dissolution of metal primarily through its adsorption on the metal surface[46].

The impedance spectra for annealed maraging steel in 0.5 M sulphuric acid without inhibitor was analysed by fitting the experimental data to the equivalent circuit model as given in Figure 6 which has been used previously to model iron/acid interface[46,47]. The impedance spectra with inhibitor was analyzed by fitting the experimental data to the equivalent circuit model as given in Figure 7 which has been used previously to model iron/acid interface[48]. The point of intersection between inductive loop and the real axis represents $(R_s + R_{ct})$. R_s represents solution resistance due to the ohmic resistances of corrosion product films and the solution enclosed between the working electrode and the reference electrode. R_{ct} represents the charge transfer resistance whose value is a measure of electron transfer across the surface and is inversely proportional to corrosion rate[49]. The constant phase element is introduced in the circuit instead of pure double layer capacitor to give more accurate fit[50]. The impedance of CPE is expressed as,

$$Z_{CPE} = \frac{1}{Y_0 (jw)^n} \quad (10)$$

where Y_0 is the magnitude of the CPE, $-1 \le n \le 1$. The

Full Paper

HF loops have depressed semicircular appearance, 0.5≤n≤1, which is often referred to as frequency dispersion as a result of the heterogeneity or roughness[46,48].

The corrosion current density I_{corr} can be calculated using charge transfer resistance R_{ct}, using Stern-Geary equation 9[49].

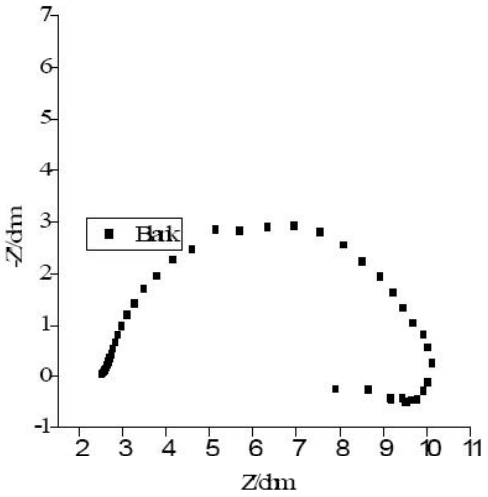

Figure 6 : Nyquist plots for annealed maraging steel specimen 0.5 M sulphuric acid without inhibitor

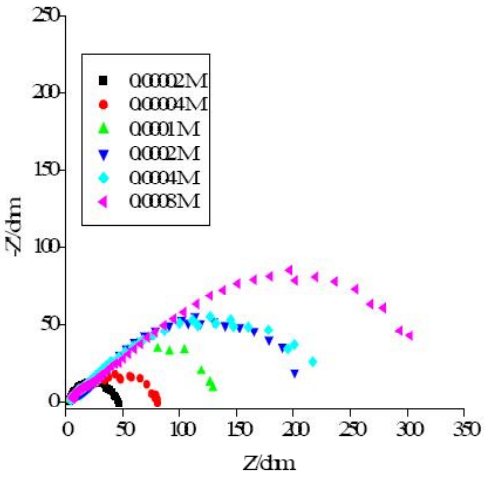

Figure 7 : Nyquist plots for annealed maraging steel specimen at various temperatures in 0.5 M sulphuric acid

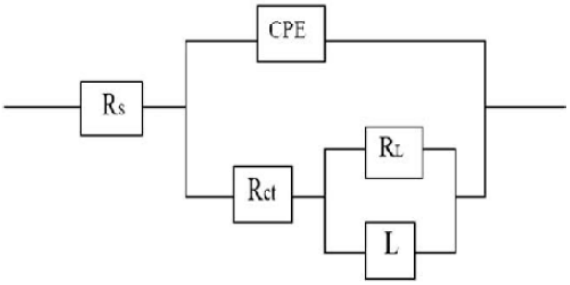

Figure 6 : Equivalent circuit used to fit experimental EIS data for the corrosion of annealed maraging steel specimen in 0.5 M sulphuric acid without inhibitor.

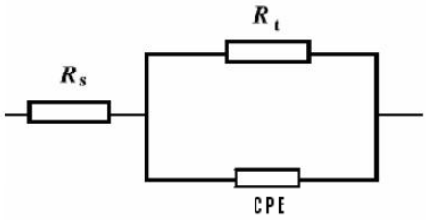

Figure 7 : Equivalent circuit used to fit experimental EIS data for the corrosion of annealed maraging steel specimen in 0.5 M sulphuric acid with inhibitor.

$$I_{corr} = \frac{b_a b_c}{2.303 A R_{ct} (b_a + b_c)} \quad (11)$$

The charge transfer resistance R_{ct} and double layer capacitance C_{dl} were determined by the analysis of Nyquist plot and their values are given in TABLE 5. The R_{ct} values obtained from Nyquist plot are in good agreement with R_p values obtained from Tafel polarization which is an evidence for the consistency between the two methods. The values of R_{ct} increases with increase in inhibitor concentration and the results indicate that charge transfer process mainly controls the corrosion process.

The double layer capacitances C_{dl}, for a circuit including CPE were calculated from the following equation[51]:

$$C_{dl} = Y_0 (w_{max})^{n-1} \quad (12)$$

where $w_{max} = 2\pi f_{max}$, f_{max} is the frequency at which the imaginary component of the impedance is maximal. According to the expression of the double layer capacitance presented in the Helmholtz model[52].

$$C_{dl} = \frac{\varepsilon \varepsilon_0}{d} S \quad (13)$$

where d is the thickness of the film, S, the surface of the electrode, ε_0 the permittivity of the air and ε is the local dielectric constant. The value of C_{dl} decreases due to adsorption of inhibitor molecules, which displaces water molecules originally adsorbed on the maraging steel surface and decreases the active surface area. The values of double layer capacitance decreases with increase in inhibitor concentration indicating that inhibitor molecules function by adsorption at the metal/ solution interface, leading to protective film on the alloy surface, and then decreasing the extent of dissolution reaction[53].

TABLE 5 : EIS data of annealed maraging steel in 0.5 M sulphuric acid in absence and presence of different concentrations of inhibitor DMBTSC.

Temperature (^{0}C)	Concentration of inhibitor (x10^{-4}) (M)	R_{ct} (ohm)	C_{dl} 10^{-6}/F
30	0.0	14.7	268
	0.2	75.0	149
	0.4	83.0	74
	1.0	90.3	38
	2.0	131.0	25
	4.0	169.0	17
	8.0	368.0	2
35	0.0	12.0	307
	0.2	67.9	160
	0.4	73.0	86
	1.0	85.0	48
	2.0	115.0	14
	4.0	150.0	23
	8.0	343.0	33
40	0.0	9.0	431
	0.2	58.0	125
	0.4	65.0	76
	1.0	80.2	28
	2.0	90.4	17
	4.0	178.0	5
	8.0	389.0	1
45	0.0	7.6	444
	0.2	48.3	81
	0.4	63.0	41
	1.0	78.0	67
	2.0	102.0	18
	4.0	243.0	5
	8.0	346.0	3
50	0.0	5.3	612
	0.2	45.0	122
	0.4	55.0	123
	1.0	82.0	58
	2.0	100.0	13
	4.0	146.0	6
	8.0	328.0	4

Scanning electron microscope studies (SEM)

The scanning electron microscope images were recorded to establish the interaction of acid medium with and without inhibitor on the metal surface using JEOL JSM-6380LA analytical scanning electron microscope. The surface morphology of the annealed samples was examined by SEM immediately after corrosion tests in 0.5 M H_2SO_4 medium. The SEM image of corroded annealed sample in Figure 8 shows degradation of alloy. Figure 9 represents SEM image of the sample after the corrosion tests in a medium of 0.5 M sulphuric acid containing DMBTSC, which clearly shows the adsorbed layer of inhibitor molecules on the alloy surface thus protecting the metal from corrosion.

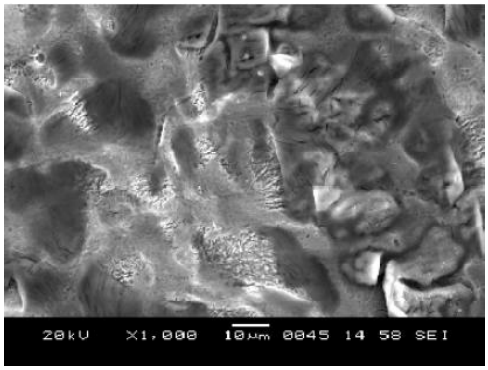

Figure 8 : SEM image of corroded annealed maraging steel after immersion in 0.5 M sulphuric acid

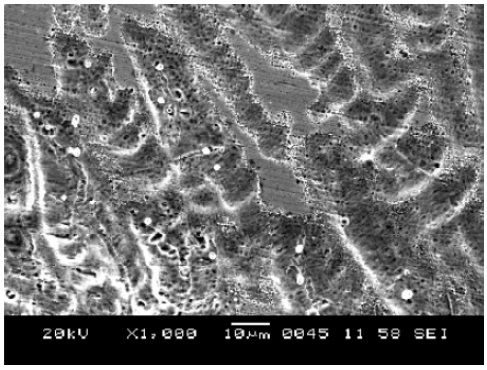

Figure 9 : SEM image of the aged maraging steel, after immersion in 0.5 M sulphuric acid containing DMBTSC

CONCLUSION

In this work, potentiodynamic polarization and electrochemical impedance methods are used to evaluate the ability of DMBTSC to inhibit corrosion of annealed maraging steel in 0.5 M sulphuric acid. The conclusions are,

1. The corrosion of annealeded maraging steel in 0.5 M sulphuric acid is significantly reduced by the addition of DMBTSC even at low concentration of inhibitor, the inhibition efficiency increases with increase in inhibitor concentration.
2. DMBTSC acts as mixed type inhibitor, affecting both anodic and cathodic reactions.
3. The adsorption of DMBTSC on annealed maraging stel surface obeys Langmuir's adsorption isotherm model for monolayer chemosorption..
4. The negative value of ΔG^0_{ads} obtained from this study indicates that these compounds are adsorbed spontaneously on the sample. The calculated Gibb's

free energy of adsorption and enthalpy of adsorption confirms the chemical nature of the adsorption.

5. SEM images revealed protection of alloy surface by DMBTSC in sulphuric acid medium.
6. The inhibition efficiency obtained from potentiodynamic polarization and EIS techniques are in reasonably good agreement.

REFERENCES

[1] K.Y.Sastry, R.Narayanan, C.R.Shamantha, S.S.Sunderason, S.K.Seshadri, V.M.Radhakrishnan, K.J.L.Iyer, S.Sundararajan; Mater.Sci.Technol., **19**, 375 **(2003)**.

[2] Kurt Rohrbach, Michael Schmidt; ASM Handbook, 10th Edn., **1**, 796 **(1991)**.

[3] D.G.Lee, K.C.Jang, J.M.Kuk, I.S.Kim; J.Mat.Proc. Tech., **342**, 162 **(2005)**.

[4] W.W.Krick, R.A.Covert, T.P.May; Met.Eng.Quart., **8**, 31 **(1968)**.

[5] S.W.Dean, H.R.Copson; Corrosion, **21**, 95 **(1965)**.

[6] G.Bellanger, J.J.Rameau; J.Nucl.Mater., **228**, 24 **(1996)**.

[7] G.Bellanger; J.Nucl.Mater., **217**, 187 **(1994)**.

[8] Data Bulletin on 18%Ni Maraging Steel, The International Nickel Company, INC, **(1964)**.

[9] J.Rezek, I.E.Klein, J.Yhalom; Corros.Sci., **39**, 385 **(1997)**.

[10] P.P.Sinha; IIM Metal News, **2**, 5 **(1999)**.

[11] S.Singh, F.Athar, A.Azam; Bioorg.Med.Chem.Lett., **15**, 5424 **(2005)**.

[12] A.R.Jalilian, R.Rowshanfarzad, M.Sabet, A.Shafiee; Appl.Radiat.Isotopes, **64**, 337 **(2006)**.

[13] Renata B.de Oliveira, Elaine M.de Souza-Fagundes, Rodrigo P.P.Soares, Anderson A.Andrade, Antoniana U.Krettli, Carlos L.Zani; Eur.J.Med. Chem., **43**, 1984 **(2008)**.

[14] Sanaa T.Arab; Mat.Res.Bull., **43**, 510 **(2008)**.

[15] B.A.Abd El-Nabey, E.Khamis, G.E.Thompson, J.L.Dawson; Surf.Coat.Technol., **28**, 83 **(1986)**.

[16] E.E.Ebenso, U.J.Ekpe, B.I.Ita, O.E.Offiong, U.J.Ibok; Mat.Chem.Phy., **60**, 79 **(1999)**.

[17] A.E.El-Shafei, M.N.H.Moussa, A.A.El-Far; Mater. Chem.Phy., **70**, 175 **(2001)**.

[18] A.E.El-Sayed, Fouda H.Abu El-Nadar, M.N.Moussa; Acta.Chim.Hung., **124**, 581 **(1987)**.

[19] J.Fang, J.Li; J.Mol.Struct.Theochem., **593**, 179 **(2002)**.

[20] L.Larabi, Y.Harek, O.Benali, S.Ghalem; Progr.Org. Coat., **54**, 256 **(2005)**.

[21] W.H.Li, Q.He, C.L.Pei, B.R.Hou; Electrochim. Acta., **52**, 6386 **(2007)**.

[22] E.S.Ferreira, C.Giancomelli, F.C.Giacomelli, A.Spinelli; Matr.Chem.Phy., **83**, 129 **(2004)**.

[23] W.H.Li, Q.He, C.L.Pei, B.R.Hou; J.Appl.Electrochem., **38**, 289 **(2008)**.

[24] E.McCafferty, N.Hackerman; J.Electrochem.Soc., **119**, 146 **(1972)**.

[25] F.Bentiss, M.Lebrini, M.Lagrenee; Corros.Sci., **47**, 2915 **(2005)**.

[26] D.D.N.Singh, R.S.Chaudhary, B.Prakash, C.V.Agarwal; Br.Corros.J., **14**, 235 **(1979)**.

[27] M.Bouklah, B.Hammouti, A.Aounti, T.Benhadda; Prog.Org.Coat., **49**, 227 **(2004)**.

[28] S.S.Abd.Ei-Rehim, Magdy A.M.Ibrahim, K.F.Khaled; J.Appl.Electrochem. **29**, 595 **(1999)**.

[29] M.Lagrenee, B.Mernari, M.Bouanis, M.Traisnel, F.Bentiss; Corros.Sci., **44**, 573 **(2002)**.

[30] M.K.Gomma, M.H.Wahdan; Mater.Chem.Phys., **39**, 209 **(1995)**.

[31] J.Marsh; Advanced Organic Chemistry, 3rd Edn., Wiley Eastern, New Delhi, **(1988)**

[32] E.E.Oguzie, V.O.Njoku, C.K.Enenebeaku, C.O.Akalezi, C.Obi; Corros.Sci., **50**, 3481 **(2008)**.

[33] Sanaa T.Arab; Mater.Res.Bull., **43**, 516, **(2008)**.

[34] E.Machnikova, H.Kenton, Whitmire, N.Hackerman; Electrichim.Acta., **53**, 6028 **(2008)**.

[35] O.Olivares, N.V.Likhanova, B.Gomez, J.Navarrete, M.E.Llanos-Serrano, E.Arce, J.M.Hallen; Appl. Surf.Sci., **252**, 2894 **(2006)**.

[36] M.Kliskic, J.Radosevic, S.Gudic, V.Katalinic; J.Appl.Electrochem., **30**, 823 **(2000)**.

[37] R.Fuchs-Godec; Colloids Surf., A.Physicochem.Eng. Aspects, **280**, 130 **(2006)**.

[38] M.Hosseini, S.F.L.Mertens, M.R.Arshadi; Corros. Sci., **45**, 1473 **(2003)**.

[39] M.Ehteshamzadeh, T.Shahrabi, M.Hosseini; Anti Corros.Meth.Mat., **53**, 296 **(2006)**.

[40] W.Durnie, R.D.Marco, A.Jefferson, B.Kinsella; J.Electrochem.Soc., **146**, 1751 **(1999)**.

[41] G.Banerjee, S.N.Malhotra; Corrosion, **48**, 10 **(1992)**.

[42] C.M.A.Brett; Corros.Sci., **33**, 203 **1992**.

[43] J.W.Lenderink, M.Liden, J.H.Wit; Electrochim. Acta., **39**, 989 **(1993)**.

[44] J.B.Bessone, D.R.Salinas, C.Mayer, M.Ebert, W.J.Lorenz; Electrochim.Acta., **37**, 2283 **(1992)**.

[45] A.Frichet, P.Gimenez, M.Keddam, Electrochim. Acta., **38**, 1957 **(1993)**.

[46] M.A.Amin, S.S.Abd.El-Rehim, E.E.F.El- Sherbini, R.S.Bayyomi; Electrochim.Acta., **52**, 3588 **(2007)**.
[47] A.Popova, E.Sokolova, S.Raicheva, M.Christov; Corros.Sci., **45**, 33 **(2003)**.
[48] Hamdy H.Hassan, Essam Abdelghani, Mohammed A.Amin; Electrochim.Acta., **52**, 6362 **(2007)**.
[49] A.El-Sayed; J.Appl.Electrochem., **27**, 194 **(1997)**.
[50] B.A.Boukamamp; Solid State Ionics, **20**, 31 **(1980)**.
[51] C.H.Hsu, F.Mansfeld; Corrosion, **57**, 747 **(2001)**.
[52] E.McCafferty, N.Hackerman; J.Electrochem.Soc., **119**, 146 **(1972)**.
[53] F.Bentiss, M.Traisnel, M.Lagrenee; Corros.Sci., **42**, 127 **(2000)**.